Optimal Power Flow Management for Grid Connected PV Systems With Batteries

Yann Riffonneau, Seddik Bacha, *Member, IEEE*, Franck Barruel, and Stephane Ploix

***Abstract*—This paper presents an optimal power management mechanism for grid connected photovoltaic (PV) systems with storage. The objective is to help intensive penetration of PV production into the grid by proposing peak shaving service at the lowest cost. The structure of a power supervisor based on an optimal predictive power scheduling algorithm is proposed. Optimization is performed using Dynamic Programming and is compared with a simple ruled-based management. The particularity of this study remains first in the consideration of batteries ageing into the optimization process and second in the "day-ahead" approach of power management. Simulations and real conditions application are carried out over one exemplary day. In simulation, it points out that peak shaving is realized with the minimal cost, but especially that power fluctuations on the grid are reduced which matches with the initial objective of helping PV penetration into the grid. In real conditions, efficiency of the predictive schedule depends on accuracy of the forecasts, which leads to future works about optimal reactive power management.**

***Index Terms*—Batteries, dynamic programming (DP), energy management, optimization, photovoltaic (PV) power systems, storage.**

I. Introduction

TO FACE the increase of the electricity demand, the reduction of fossil fuel resources and the need of reducing CO_2 emissions, grid connected renewable power systems have gained outstanding interest. In this context, wind and photovoltaic (PV) generation appear as the most promising issues. Especially, PV is highly developing in the building energy sector for which it is particularly relevant. This progression clearly appears in Fig. 1 through distributed grid connected systems increase. According to the incentive policies to help PV development and taking into account the reduction of the costs, expansion of grid connected PV systems is expected to continue in the next decade. Because of its intermittent and irregular nature, PV generation makes grid management harder. Consequently, for some authors [2], [3] , PV production into the grid is considered to be limited.

Manuscript received September 13, 2010; revised January 04, 2011; accepted January 31, 2011. Date of publication February 17, 2011; date of current version June 22, 2011. This work was supported in part by the Agency of Environement and Energie Management (ADEME), France.

Y. Riffonneau and S. Bacha are with the Univeristy Joseph Fourier, Grenoble Electrical Engineering Laboratory (G2ELAB), 38402 St. Martin d'Hères, France (e-mail: yann.riffonneau@g2elab.grenoble-inp.fr; Seddik.Bacha@g2elab.inpg.fr).

F. Barruel is with the National Solar Energy Institute (INES), Bâtiment Lynx 73377 Le Bourget du Lac, France (e-mail: franck.barruel@cea.fr).

S. Ploix is with the Grenoble Institute of Technology, G-SCOP Laboratory, Viallet-38031 Grenoble, France (e-mail: stephane.ploix@inpg.fr).

Digital Object Identifier 10.1109/TSTE.2011.2114901

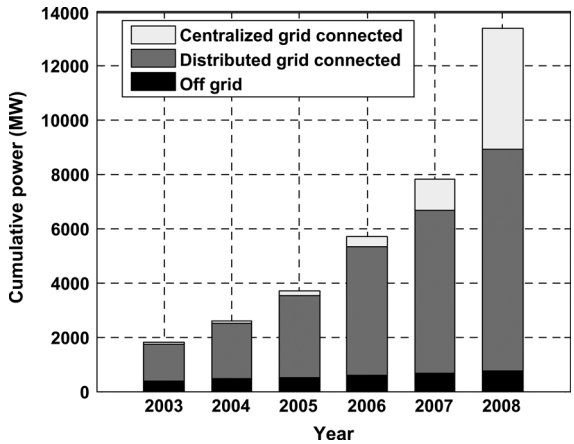

Fig. 1. Cumulative PV systems installed in the IEA country [1].

One of the major challenges for PV systems remains in the matching of the intermittent energy production with the dynamic power demand. A solution is to add a storage element to these nonconventional and intermittent power sources [4], [5] . In this case, the hybrid system, composed of a PV generator, local loads, electricity storage, and the grid, can perform many applications [6]. However, the integration of grid connected storage is currently limited by two constraints.

1) Regulations: At the moment, grid connected storage in an end-user installation is forbidden to prevent abusive benefit from electricity purchase of incentive feed-in tariff attributed to PV power. However, it is expected that regulations will become more flexible as in the example of the new German feed-in law from EGG [7].

2) Power Flow Management: An electrical storage element generates expensive investment and operation costs with strong operating constraints. In this context and considering that subventions are restricted in the short-term future, the objective is to reduce operation costs by managing the power flows in the system. It is an optimization problem that consists of optimizing the use of the storage, the use of the PV source, and to match the local production with the local consumption.

This paper deals with power flows management for grid connected PV systems with storage (GPVS) with a focus on optimal scheduling. Section II presents the analyzed system. It describes the structure of the power flow supervisor proposed and introduces the power management and optimization tools. Section III presents the modeling of the components of the system. Section IV describes the optimization method and its application to solve the power management problem. Section V carries out results from simulations in a specific context. Section VI presents experimental application in real condition

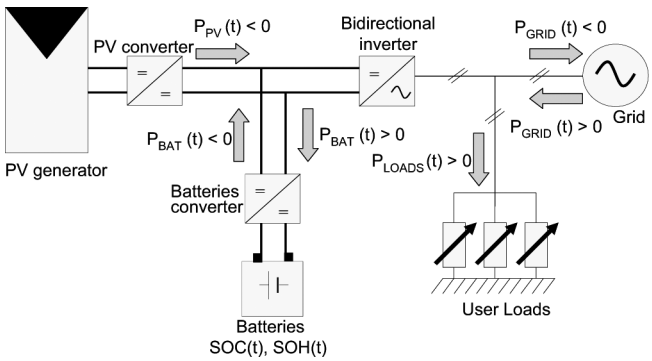

Fig. 2. Power direction and sign convention in the system studied.

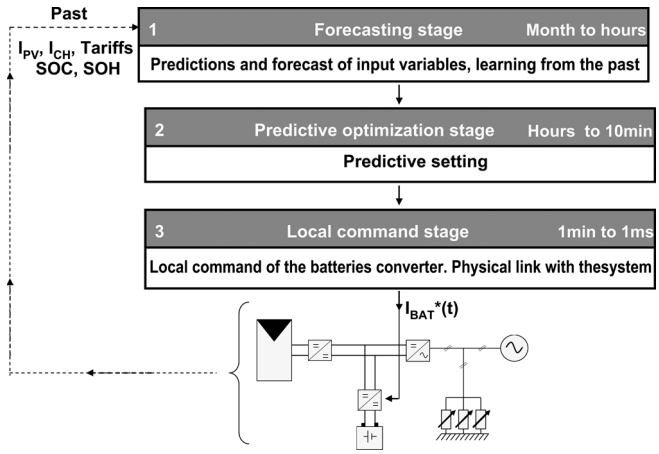

Fig. 3. Proposed structure of the power flow management supervisor.

and Section VII concludes the study and introduces the reactive management concept.

II. System Architecture

A. Presentation of the System

A scheme of the studied system is presented in Fig. 2. The different power directions are represented. The sign convention in Fig. 2 is used as a reference throughout the whole paper. The main components of the hybrid system are the PV generator, the batteries' energy storage, the user loads, the distribution grid, and the electronics power converters. The parameters $\ll \mathrm{SOC} \gg$ and $\ll \mathrm{SOH} \gg$ are, respectively, the values of the state of charge and state of health of the batteries, whose calculations are detailed in Section III.

According to the sign convention, the laws of physics require the power balance in the system described by

$$P_{\mathrm{GRID}}(t) = P_{\mathrm{PV}}(t) + P_{\mathrm{BAT}}(t) + P_{\mathrm{LOADS}}(t). \quad (1)$$

The first limitations on the operation of the system are the physical constraints formulated by (1)–(4). These constraints are set to limit the batteries' degradation and ageing

$$\mathrm{SOC}^{\min} \leq \mathrm{SOC}(t) \leq \mathrm{SOC}^{\max} \quad (2)$$

$$P_{\mathrm{BAT}}^{\min} \leq P_{\mathrm{BAT}}(t) \leq P_{\mathrm{BAT}}^{\max} \quad (3)$$

$$\mathrm{SOH}(t) \geq \mathrm{SOH}^{\min}. \quad (4)$$

Another limitation is imposed by the usage of the system: as mentioned before, where the target is peak shaving, such as the power exchange with the grid, is limited to a maximum threshold value as formulated by

$$P_{\mathrm{GRID}}(t) \leq P_{\mathrm{GRID}}^{\max}. \quad (5)$$

Performing peak shaving with the PV generator and the storage helps the penetration of PV electricity into the grid. First, it makes the grid management easier as the load profile is smoothed. Second, it reduces the CO_2 emissions as the peak power is generally supplied by rapid startup power plants that are important CO_2 producers.

B. Power Flow Supervisor

To perform optimal power flow management, a supervisor whose structure is presented in Fig. 3 is proposed. It is composed of three stages that are described below. The input data and the time range of the output data of each stage are shown.

The forecasting stage provides the necessary predicted input data to the optimization stage. Because the more reliable the forecasts, the more efficient the power management, many techniques to minimize the prediction error have been developed [8], [9]. The forecasts are calculated from months to hours.

During the predictive optimization stage, the power flow management problem is solved. It is called predictive optimization as the resolution is built on the *a priori* knowledge of the future from the forecasts. The step time of this stage is from hours to 10 min.

The local control stage is in charge of assigning the command to the power electronic elements in order to apply the power flow schedule from the optimization stage. This stage operates within a time scale from 1 min to 1 ms.

This study focuses on the predictive optimization stage. The forecast data (irradiance $(G_T[\mathrm{W/m^2}])$, ambient temperature $(T_{\mathrm{amb}}[^\circ\mathrm{C}])$, user loads consumption profile $(P_{\mathrm{LOADS}}[\mathrm{W}])$, and electricity grid price [€/kWh]) are considered known. To find out how to solve the power management problem, a quick overview of the suitable tools is proposed in Section II-C.

C. Power Management and Optimization Tools

The method to perform power management optimization is chosen according to the nature of the problem (component, constraints, and performance index). The main purpose of this work is to find the power flow scheduling that minimizes the energy bill of the owner of the system over the studied period. The input data (irradiance, ambient temperature, user's load consumption profile, and electricity grid price) are variable and their prediction is uncertain. It is a constrained problem in a finite horizon because the length of the studied period is known. The components (powers in the system) are "*a priori*" continuous and the constraints and objective function are not particularly derivable or linear. The proposed overview is inspired from the fields of stand-alone PV systems, grid connected PV systems, and hybrid electric vehicles (HEVs).

A ruled-based management may be applied. Power flows are managed according to a set of case-triggered rules built from heuristic knowledge [10]. Operation of the system is restricted

to the developed rules that have to ensure that the constraints are satisfied, but optimization is not guarantee [11]–[13]. A first step to optimization is to determine the rules from a fuzzy logic controller such as in [14] and [15]. It is also important to notice that the development of a set of triggered rules becomes quickly fastidious because of the number of possibilities.

As a first step, a nonoptimal ruled-based algorithm has been developed. It guarantees operation of the system with respect to the constraints. The ruled-based powers schedule will be used as the reference to compare the performances of the optimization algorithms.

The most commonly used techniques for optimization are linear programming (LP) [16]–[18], dynamic programming (DP) [18]–[20], and quadratic programming by formulating the problem in relaxing form with the Lagrangian multipliers [18], [21], and [23].

According to its name, LP implies that the problem is linear. In our case, to formulate the problem on linear form, it is necessary to integrate a binary variable and so a discrete value variable [17]. In this case, LP cannot solve the problem and mix integer linear programming (MILP) has to be used, such as in [16]. MILP gives very good results as the problem is correctly formulated and demands low computing resources. However, the main limitation is the need of a specific mathematical solver [16]. In the perspective of future work, it is interesting to notice that LP and MILP become also very unsuitable techniques for reactive optimization (modification) of the predictive strategy according to actual measurement. Actually, in this case, the problem has to be solved again over the period left at each unpredicted disturbance with the forecast (important computation time).

DP is a graph-based technique corresponding to the shorter path algorithms. The advantage is that the performance index and the constraints can hold all the natures (linear or not, differential or not, convex or concave, etc.) and no specific mathematical solver is needed. DP can also be used for reactive optimization by correcting the predictive strategy at each unpredicted disturbance according to the real values. As DP works on discrete or sequential problems, evolution of the system has to be decomposed into several steps [20] and [21] . A similar approach has been used in [22] for deterioration and maintenance model of wind turbines. The weakness of this technique is its high memory needs when the studied period is long and discretized with a small time step [10]. However, it is not problematic if the computation parameters are well chosen. In addition, the computation time can be reduced by appropriate modifications.

Quadratic programming gives very good results since the problem is formulated in a relaxing form through the Lagrangian multiplier. However, this method needs the objective function to be convex (or concave), which generally implies simplifications of the problem [18], [21] . In [21], it is carried out that these simplifications are the main origins of the errors between the ideal and the calculated solution. Also, quadratic programming is suitable only for a small problem (less than 50 variables) and works only with continuous variables. This technique is a strong candidate for reactive optimization and the most used in HEV application as in [23] and [24].

From this overview, DP has been chosen to perform optimal power flow management. The Bellman algorithm, detailed in Section IV, has been chosen.

III. System Modeling

In this section, we present the modeling of the PV generator, the batteries, and the power converter. The grid is considered as a perfect power source or power sink.

A. PV Generator

The PV generator has been modeled by a linear power source according to the ambient temperature and the irradiance level [25], [26] . Output power of the total generator at the maximum power point (MPP) is obtained from (6) and (7), where parameters are obtained from information available from the manufacturer data sheets [nominal operating cell temperature (NOCT) and standard test condition (STC)]

$$P_{\mathrm{PV}} = \left[P_{\mathrm{PV,STC}} \times \frac{G_T}{1000} \times [1 - \gamma \times (T_j - 25)]\right] \times N_{\mathrm{PVs}} \times N_{\mathrm{PVp}} \quad (6)$$

where P_{PV}, $P_{\mathrm{PV,STC}}$, G_T, γ, T_j, $N_{\mathrm{PV\_S}}$, and $N_{\mathrm{PV\_P}}$ are the generator output power at the MPP, the rated PV power at the MPP and STC, the irradiance level at STC, the power temperature coefficient at MPP, the cell temperature, and the number of modules in series and in parallel that composed the generator, respectively. The STC measure conditions are $T_{j,\mathrm{STC}} = 25\ ^{\circ}\mathrm{C}$, $G_{T,\mathrm{STC}} = 1000\ \mathrm{W/m^2}$, and wind speed of 1 m/s.

The cell temperature Tj is obtained from (7), where T_{amb} and NOCT are the ambient air temperature and the NOCT. The NOCT measurement conditions are $T_{\mathrm{amb,NOCT}} = 20\ ^{\circ}\mathrm{C}$, $G_{T,\mathrm{NOCT}} = 800\ \mathrm{W/m^2}$ and wind speed of 1 m/s

$$T_j = T_{\mathrm{amb}} + \frac{G_T}{800} \times (\mathrm{NOCT} - 20). \quad (7)$$

In this paper, the PV generator is composed of polycrhistalline modules with 72 cells in series that are all considered to be at the same temperature. The temperature coefficient "γ" of the modules is $0.043\%/^{\circ}\mathrm{C}$, the "NOCT" is $45.5\ ^{\circ}\mathrm{C}$, the "$P_{\mathrm{PV,STC}}$" of each module is 165 W.

B. Batteries

This study has been performed with flat plate lead acid batteries. The model presented corresponds to this technology.

1) State of Charge (SOC): Estimation of lead acid batteries' SOC is not obvious and it is still the subject of many studies [27]–[29]. The specific SOC calculation from [30] and [31] has been chosen for this study. It takes into account the variation of the quantity of charge in the process as a function of the current rates and the ambient temperature. As this model has already been used and described in [32], presentation of calculation in this paper is restricted to (8) and (9), where "$C(t)$" is the batteries' capacity at each instant, "$C_{\mathrm{ref}}(t)$" is the capacity of reference, $Q(t_0)$ is the initial quantity of charge, and $Q_c(t)$ and $Q_d(t)$ are, respectively, the quantity of charge exchange during the charge and discharge process. The capacity of reference "$C_{\mathrm{ref}}(t)$" varies according to the ageing process express

by (11) and (12). For more details, the reader is encouraged to read [30]–[32]

$$\mathrm{SOC} = \frac{C(t)}{C_{\mathrm{ref}}(t)} \tag{8}$$

$$C(t) = Q(t_0) + Q_c(t) + Q_d(t). \tag{9}$$

2) Ageing Process: State of Health (SOH) of batteries is defined by (10) where $C_{\mathrm{ref,nom}}$ is the nominal capacity of reference available from the manufacturer data sheet [31]

$$\mathrm{SOH}(t) = \frac{C_{\mathrm{ref}}(t)}{C_{\mathrm{ref,nom}}}. \tag{10}$$

Degradations of the performances of batteries during the ageing process have been modeled by [31] and [33]. It is represented as losses of capacity of reference that are considered linear according to the depth of discharge of batteries [34], [35] . From experimental results performed at the INES institute and presented in [33], linear ageing coefficients "Z" for different battery technologies have been carried out. The coefficient "Z" has a value of 3.10^{-4} for lead acid technology.

At each step size, if the battery's operation is a discharge, the new capacity of reference is obtained by (11) from capacity losses calculated with (12)

$$C_{\mathrm{ref}}(t) = C_{\mathrm{ref}}(t - \Delta t) - \Delta C_{\mathrm{ref}}(t) \tag{11}$$

$$\Delta C_{\mathrm{ref}}(t) = C_{\mathrm{ref,nom}} \times Z \times [\mathrm{SOC}(t - \Delta t) - \mathrm{SOC}(t)]. \tag{12}$$

Replacing $C_{\mathrm{ref}}(t)$ in (10) by expressions (11) and (12) and the SOH according to the SOC variation is expressed by

$$\mathrm{SOH}(t) = \frac{C_{\mathrm{ref}}(t - \Delta t)}{C_{\mathrm{ref,nom}}} - Z \times [\mathrm{SOC}(t - \Delta t) - \mathrm{SOC}(t)]. \tag{13}$$

Equation (12) is always positive as it is computed only in discharge. The new capacity of reference calculated by (11) is replaced into the SOC estimation (8) such as ageing involves performance modification.

3) Voltage ("V_{BAT}"): As a simple representation of the global behavior, the voltage of batteries has been considered linear in charge and in discharge as a function of the SOC (calculated as time integration of the current). From linear interpolation of experimental results carried out at the INES institute, the voltage of batteries in charge and discharge is determined by (14) and (15), where "N_{BAT_S}" is the number of batteries of 12 V connected in series. Experimental results and linear interpolation are presented in Fig. 4

$$V_{\mathrm{BAT}}(t) = [12.94 + 1.46 \times \mathrm{SOC}(t)] \times N_{\mathrm{BAT}\_S} \tag{14}$$

$$V_{\mathrm{BAT}}(t) = [12.13 - 1.54 \times (1 - \mathrm{SOC}(t))] \times N_{\mathrm{BAT}\_S}. \tag{15}$$

This modeling is elementary but appropriate for this application as it is simple and significantly representative of the behavior in the range of operation conditions of the system. The battery's power "P_{BAT}" in (1) and (3) is obtained by multiplying the battery's voltage modeled here by the input or output battery's current.

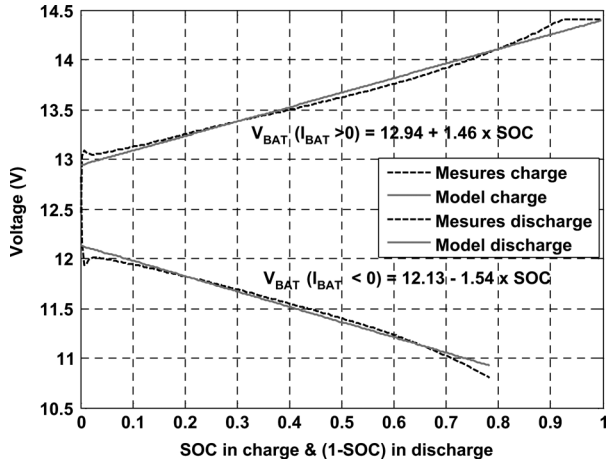

Fig. 4. Experimental measures and linear modeling of the charge and discharge voltage as a function of SOC (12-V lead acid battery and IBAT is constant at a rate of 5 h).

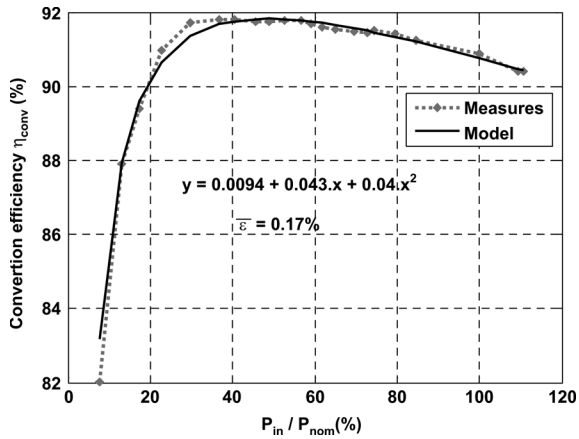

Fig. 5. Measures and identified converter efficiency curves [36].

C. Converter Efficiency

The power electronics converters have been modeled according to their efficiency as a function of the input normalized power, where losses are assumed to be a quadratic function. The conversion efficiency formulation (16) is carried out from a quadratic interpolation of an experimental curve generated at the INES institute [36]

$$\eta_{\mathrm{conv}} = 1 - \frac{1}{\mathrm{In}} \times (0.0094 + 0.043 \times \mathrm{In} + 0.04 \times \mathrm{In}^2) \tag{16}$$

where "In" is the normalized input power of the converter $(P_{\mathrm{in}}/P_{\mathrm{conv\_rated}})$.

Fig. 5 shows the efficiency curve measured and modeled from identification. The average error is 0.17%. Calculation of efficiency with (16) is applied on the PV converter, the batteries' converter and the dc/ac and ac/dc conversion of the bidirectional converter.

IV. DP and Power Flow Management

This section details the optimization stage procedure of the supervisor presented in Fig. 3. The first subsection summarizes the problem to be solved with the constraints and the objective

function. The second subsection presents the application of the DP to solve the problem.

A. Problem Formulation

The system studied is presented in Fig. 2 in Section II and the operating constraints, defined by (1)–(5) are summarized as follows:

$$P_{\mathrm{GRID}}(t) = P_{\mathrm{PV}}(t) + P_{\mathrm{BAT}}(t) + P_{\mathrm{LOADS}}(t) \quad (17)$$

$$\mathrm{SOC}^{\min} \leq \mathrm{SOC}(t) \leq \mathrm{SOC}^{\max} \quad (18)$$

$$P_{\mathrm{BAT}}^{\min} \leq P_{\mathrm{BAT}}(t) \leq P_{\mathrm{BAT}}^{\max} \quad (19)$$

$$\mathrm{SOH}(t) \geq \mathrm{SOH}^{\min} \quad (20)$$

$$P_{\mathrm{GRID}}(t) \leq P_{\mathrm{GRID}}^{\max}. \quad (21)$$

Constraint (17) comes from the law of physics, constraints (18)–(20) are physical constraints to limit the batteries' degradations and ageing, and constraint (21) corresponds to the peak shaving application.

It is assumed that the loads are not controllable but have to be supplied at any time. Forecasts on load consumption are used to find the power management strategy.

The objective function of supplying the user loads at the best cost is expressed by (22). It amounts to minimizing the final value of the cash flow "CF" over the entire studied period. The cash flow is composed of the cash received "CR" and the cash paid "CP"

$$\mathrm{Min}(\mathrm{CF}) = \mathrm{Min} \sum_{t=t_0}^{T} [\mathrm{CR}(t) + \mathrm{CP}(t)]. \quad (22)$$

The cash received is the benefits made from any electricity operation related to an agreement with the grid operator. Generally, it corresponds to the benefits from selling PV electricity. However, some new agreements, such as [7], enable us to make benefits from the self-consumption of energy from the PV generator. In this case, cash received corresponds to both benefits. The cash paid corresponds to all the operation costs of the system. In our case, it is composed of the cost of electricity purchase from the grid and of the ageing cost of batteries. As a very important cost; ageing of batteries is taken into account in the optimization process through the calculation of the SOH. Details of ageing cost calculation are presented in Section IV-B. The cash received or paid is a power (kW) multiplied by a price (€/kW) so its value is directly related to the power flow management. The power sign convention in Fig. 2 has been defined such that the cash received is negative and the cash paid is positive.

It is important to note that constraint (21) is not necessarily strict such that if it is not satisfied, the solution is not rejected but a penalty cost is applied. In this way, all the solutions are taken into account which gives more flexibility to the system.

B. Dynamic Programming

DP has been used to solve the optimization problem. Definitions and fundamental principles may be found in [37]. The problem is formulated as a system evolution divided in a multistage decision process. At any time "t," the state of the system is determined by a set of quantity called states variables. In our case, the state of the system corresponds to the SOC of the batteries, discretized with a step size of "$\delta\mathrm{SOC}$." At each step time "Δt," the batteries can take any of the discretized value $\delta\mathrm{SOC}$ in a range that guarantees constraint (18). Fig. 6 illustrates an example of an SOC space for three time steps. All possible trajectories from the initial state at the initial time to all the allowed states at the final time are represented.

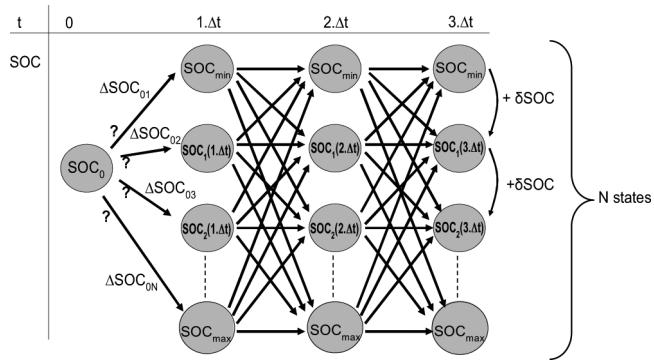

Fig. 6. Batteries' SOC space and the possible trajectories for the case of three-step time.

A transition between two states during one time step corresponds to a SOC variation written "$\Delta\mathrm{SOC}$." As each $\Delta\mathrm{SOC}$ corresponds to a battery's power value, the constraint (19) is translated in terms of SOC variation as presented by (23). This reduces the computation time to check the satisfaction of the constraints

$$\Delta\mathrm{SOC}^{\min} \leq \Delta\mathrm{SOC}(xi, xj, t) \leq \Delta\mathrm{SOC}^{\max}. \quad (23)$$

For each $\Delta\mathrm{SOC}$, first the "P_{BAT}" and "P_{GRID}" are calculated according to the *a priori* knowledge of the loads consumption "P_{LOADS}" and the PV availability "P_{PV}," and second, the corresponding CF value is obtained. As an example, if the cash received comes only from feed-in PV power, the corresponding CF of one SOC transition is expressed by (24), where "FiT" is the feed-in tarif, "EgP" is the electricity grid price, and "BrC" is the battery's replacement cost defined as follows:

$$\begin{aligned}\mathrm{CF}(\Delta t) &= \mathrm{CR}(\Delta t) + \mathrm{CP}(\Delta t) \\ &= \left[P_{\mathrm{GRID}}(\Delta t) \times \mathrm{FIT}(\Delta t) \times \Delta t \right]_{P_{\mathrm{GRID}}(\Delta t) \leq 0} \\ &\quad + \left[P_{\mathrm{GRID}}(\Delta t) \times \mathrm{EgP}(\Delta t) \times \Delta t + \mathrm{BrC}(\Delta t) \right]_{P_{\mathrm{GRID}}(\Delta t) > 0}.\end{aligned} \quad (24)$$

The replacement cost is the translation of the degradation of the batteries. It is calculated by (25) according to the variation of SOH during each time step. Replacing SOH by its formulation (13); the SOH variation is expressed by (26) and is a linear function according to the SOC variation and the ageing coefficient. The SOH decreases only during the discharge process so expressions (25) and (26) are negative as it is calculated only in discharge

$$\Delta\mathrm{SOH}(xi, xj, t) = \mathrm{SOH}_{xi}(t - \Delta t) - \mathrm{SOH}_{xj}(t) \quad (25)$$

$$\Delta\mathrm{SOH}(xi, xj, t) = Z \times [\mathrm{SOC}_{xi}(t - \Delta t) - \mathrm{SOC}_{xj}(t)]. \quad (26)$$

The replacement cost BrC is calculated by (27) such as it satisfies (28). The sign of the SOH variation is inverted to make the BrC positive

$$\mathrm{BrC}(xi,xj,t) = \mathrm{BiC} \times \left(\frac{-\Delta \mathrm{SOH}(xi,xj,t)}{1-\mathrm{SOH}_{\min}} \right) \quad (27)$$

$$\sum_{\substack{t \text{ such as SOH}=\mathrm{SOH}_{\min} \\ t \text{ such as SOH}=1}} \mathrm{BrC}(t) = \mathrm{BiC}. \quad (28)$$

Formulated as above, the problem is to find the optimal sequence of SOC transition from the initial time to the final time that achieves the final state from the initial state with the lower CF value. To solve this shorter path problem, the Bellman's algorithm, described in [37] and [38], has been used. Fig. 7 shows the flowchart of the algorithm with the detailed computation of the weight of the arcs. An example and results are presented in Section V.

V. Simulations and Results

A. Context and Parameters Values

The optimization has been performed in the economical context of a French standard electricity price. For instance, to illustrate the upcoming economical context, no subvention for the PV power is considered: The energy fed into the grid is purchased at the same price as the electricity sold to the final consumer. It is assumed it is allowed to feed the grid with power from batteries, but it is not paid. However, it is allowed to charge the batteries from the grid. Fig. 8 is a scheme of the system with the energy meters.

In this context, the cash flow paid and received are expressed by (29), (30), and (31), where "FiT" is the feed-in tariff, "EgP" is the electricity grid price, and "E_{ci}" is the energy measured with the meter "Ci." Calculation of the cash received by (30) and (31) guaranties the purchase of only the power fed into the grid from the PV generator. According to the power's sign convention defined in Fig. 2, the cash received expressed by (29) is negative

$$\mathrm{CP}(t) = E_{C3}(t) \times \mathrm{EgP}(t) + \mathrm{BrC}(t). \quad (29)$$

Since $E_{C2} \leq E_{C1}$

$$\mathrm{CR}(t) = E_{C2}(t) \times \mathrm{FiT}(t) \quad (30)$$

else

$$\mathrm{CR}(t) = E_{C1}(t) \times \mathrm{FiT}(t). \quad (31)$$

The constraints are expressed by (17)–(21) and the objective function is (22), according to the values of Table I.

Constraint (19) is expressed in terms of "ΔSOC" as (23). Constraint (21) is not strict, such that if it is not satisfied, the grid penalty factor "GpF" is applied to the over power according to (32).

If $P_{\mathrm{GRID}}(t) > P_{\mathrm{GRID}}^{\max}$:

$$\mathrm{CP}(t) = \mathrm{EgP} \times [P_{\mathrm{GRID}}^{\max} + (P_{\mathrm{GRID}}(t) - P_{\mathrm{GRID}}^{\max}) \times GpF] \times \Delta t. \quad (32)$$

The input values are forecast coming from meteorological data ("G_T"&"T_{amb}"), forecasts of the loads consumption profile ("P_{LOADS}"), and the electricity prices ("EgP"&"FiT"). Experimental measurements performed at the INES institute in 2007 are used as meteorological forecasts. Similarly, the forecasts on load consumption are measurements achieved in Chambéry (France) for a family of three people with an off-peak/on-peak electricity agreement and an electrical heating system. According to this agreement, the load profile carries out high fluctuation and power peaks. This profile has been chosen because it is a standard situation in France. As the load profile is already optimized according to off-peak/on-peak electricity prices, the simulation and optimization presented below have been performed in the context of a single fixed electricity price. The size of the system is set to the value provided by Table II and has been determined with the sizing method proposed in [39].

B. Results and Graph

The simulation has been carried out in 24 hours for the 22nd of February as an exemplary day to figure out optimization results. The DP algorithm whose flowchart is shown in Fig. 6 has been developed with the Matlab software. Regarding the results presented here, the computation time is less than one minute.

The power scheduling obtained with the DP optimization algorithm is presented in Fig. 9. In this figure, positive battery power corresponds to a charge and negative power to a discharge. Positive grid power corresponds to a consumption and negative grid power to feed-in power. Fig. 10 shows the SOC variation corresponding to the power schedule of Fig. 9.

As expected, the power exchanged with the grid is maintained to the maximum limit. The batteries' operation is managed to satisfy the constraints regarding the lower cost for the owner of the system.

As an SOC of 50% is not enough to guarantee peak shaving later in the day, the batteries are charged in the morning. Charge is completed from the grid because there is no PV production. As shown in Fig. 10, the batteries are fully discharged after the first peak loads. The charge process is not directly launched as there is a period to wait for more PV production. The batteries are charged as much as possible with the PV power as it is the optimal operation according to the economical context. In this case, the use of the PV power is considered to be optimal. The second peak load is in priority shaved with PV power and batteries are used only when the solar production is not sufficient.

With this management, it is observed in Fig. 9 that the feed-in power is minimized, which reduces the power flow fluctuation on the grid. As shown in Fig. 10, the SOC of the batteries returns to its initial value at the end of the day. The initial SOC of 50% (and final also) has been chosen such that it gives the maximum of flexibility to the power management of the next day and so in a day-ahead supervision.

The results obtained with DP are compared with the ones obtained with a simple ruled-based algorithm presented in Figs. 11 and 12. The rules are defined such as the batteries are maintained to their maximum SOC to guarantee peak shaving. As there is no forecasting, charge of the batteries is performed with the first available power source (PV or grid) according to the constraints: the PV power is in priority used to supply the loads.

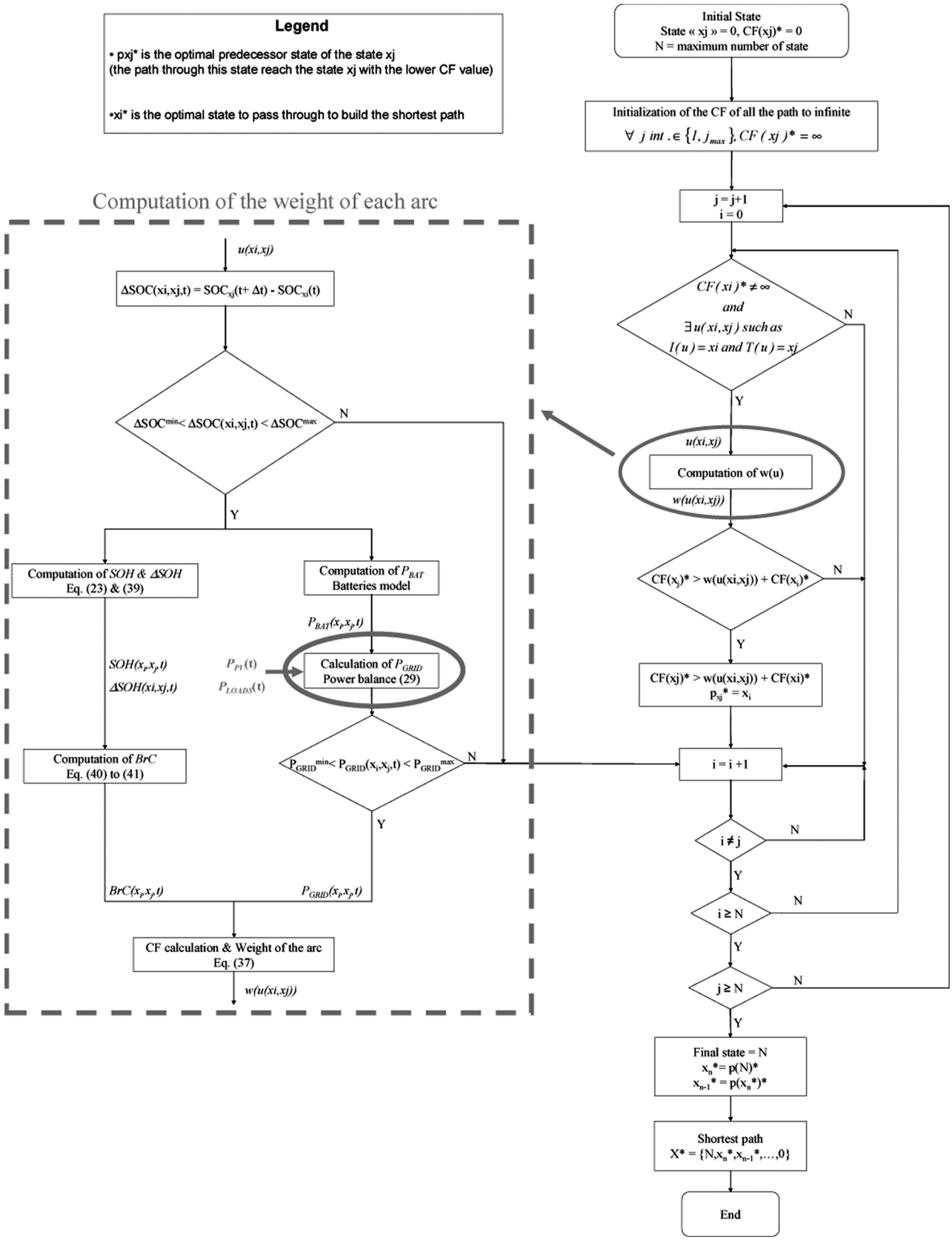

Fig. 7. Flowchart of DP algorithm developed for power management.

The ruled-based algorithm works with continuous values of the components as the DP needs discrete values, which explains the differences in power profiles, in SOC variation, and the "steps" of the batteries' power that appear in Fig. 9.

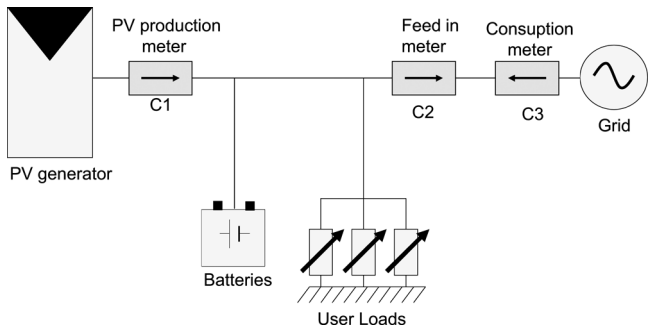

Fig. 8. Scheme of the system with the energy meters.

TABLE I
SIMULATION PARAMETER VALUES

T	24	(h) Period studied
Δt	10	(min)
δSOC	0.01	
SOC_{min}/SOC_{max}	0.2 / 0.9	
$SOC(t_0)$	0.5	
$\Delta SOC^{min}/\Delta SOC^{max}$	-0.7 / 0.7	(during 1h)
$P_{GRID}{}^{max}$	3	(kW)
BiC	150	(€/kWh)
EgP	0.11	(€/kWh)
FiT	0.11	(€/kWh)
GpF	10	

TABLE II
SIZE OF THE ELEMENTS OF THE SYSTEM STUDIED

$P_{LOADS}{}^{max}$	4	(kW)
P_{PVp}	1.6	(kW), PV peak power of the generator
N_{PV_S}	5	Number of PV modules in series
N_{PV_P}	2	Number of PV modules in parallel
$C_{ref,nom}$	100	(Ah) Capacity of the total storage
$V_{bat,nom}$	12	(V) Voltage of 1 battery
N_s	10	Number of batteries in series
N_p	1	Number of batteries in parallel

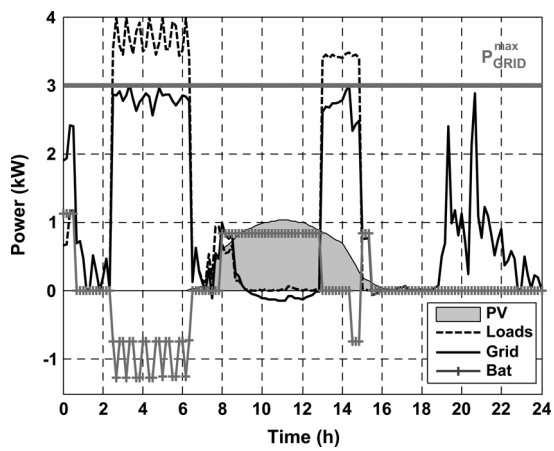

Fig. 9. Power schedule with DP optimization.

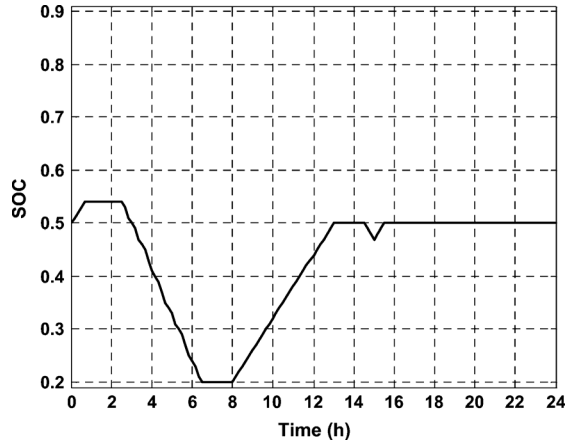

Fig. 10. SOC schedule of batteries with DP optimization.

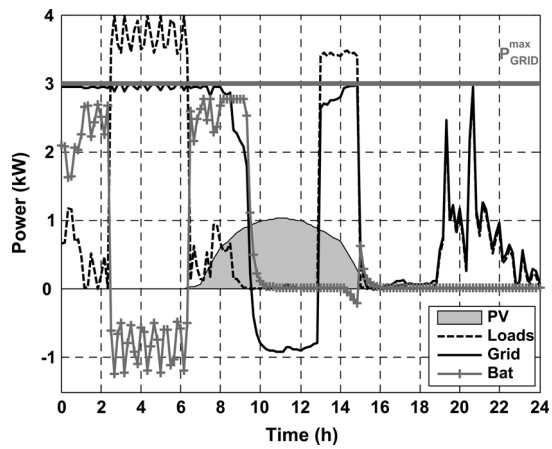

Fig. 11. Power schedule with simple ruled-based management.

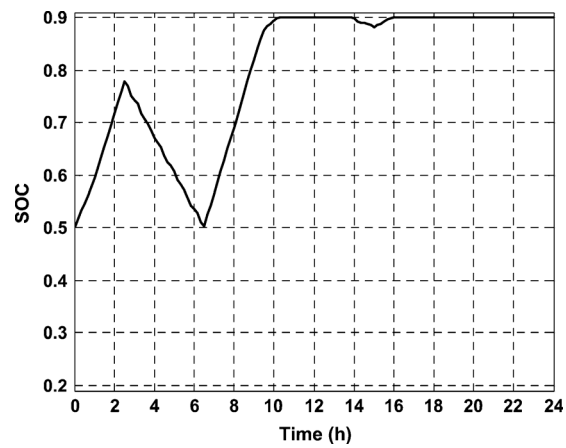

Fig. 12. SOC schedule of batteries with ruled-based management.

The ruled-based algorithm is interesting because the power exchange with the grid is maintained to the maximum bound and the constraints are satisfied. The two figures carry out that the batteries are charged as soon as possible with the first available source. Consequently, the solar energy produced during the most powerful period is not locally used but is injected into the grid and creates power fluctuations. In this case, it is considered that the use of the solar power is not optimized. Because there is no forecasting, the charge at the beginning of the day is the consequence of the main rule and not a prediction of future needs. As the rule is to keep the batteries as full as possible, the final SOC is maximum and different than the initial one. In this condition, the flexibility of the management of the next day is restricted as the batteries are full and the charge operation will

TABLE III
FINAL VALUE OF THE OBJECTIVE FUNCTIONS FOR EACH POWER MANAGEMENT

	DP	Ruled-based
Final CF (€)	9.50	10.95

not be possible. This way, it is considered that the ruled-based management is not the most suitable for day-ahead supervision.

The final value of the objective function (cash flow) for the DP optimization and the ruled-based management is presented in Table III. The DP algorithm gives a lower value as it is an optimization. Gains with DP optimization are around 13% higher than with the ruled-based management but it is very dependent of the economical context.

VI. EXPERIMENTATION OF THE MANAGEMENT IN REAL CONDITIONS

The optimal management proposed in this study is based on the forecasts on the meteorological conditions ("T_{amb}" and "E" for the PV production) and on the loads profile consumption. According to this important assumption, this section studies the power flows in the system when the predictive power scheduling, from the predictive optimization, is applied in real conditions. In this objective, the DP algorithm has been implemented into a microcontroller and tested in real-time operation. This has been realized on the experimental bench "RTLab" that is presented in Section VI-A and in [40] and [41]. To evaluate the interest of optimal predictive scheduling, the results are compared with the ruled-based strategy, also implemented in the microcontroller and applied in the same conditions. At the moment, studies in real conditions are limited to the case of a different PV power production from the forecasts. The loads power profile is considered *a priori* perfectly known. The real conditions have been simulated as representative perturbations on the forecast according to the real behavior of the meteorological parameters.

A. Presentation of RTLab and Implementation of the Management

The model of the system presented in the previous sections has been implemented in the RT-Lab HILBox 4U digital system. This system provides tools for running simulations of highly complex models on a multiprocessor architecture communicating via ultralow-latency technologies to achieve high-speed computations [40]. RT-Lab handles synchronization and real-world interfacing using fast input/output (I/O) boards and data exchanges for hardware-in-the-loop/power-in-the-loop (HIL/PIL) applications. Its architecture consists in an eight-processor (two Intel Xeon quad-core 2.33 GHz) machine exchanging data on a shared memory. Their PCI bus is connected to the digital and analog I/O system via an FPGA controller. There are 2×16, 16-bit analog inputs and outputs, with a high update rate of 1 μs. The digital interface consists of 2×16 I/O allowing a data rate of 1 MHz. The model of the system has been implemented in Matlab/Simulink software where specific blocks for RTLab operation have been added. These blocks are necessary to perform fixed time step simulation involving dynamics and discrete events asynchronous with respect to the simulation clock. The optimization algorithm is integrated in Simulink as an S-function such that it can be implemented in the microcontroller. The complete model is then compiled, loaded into the above-described hardware, and executed in real time [41].

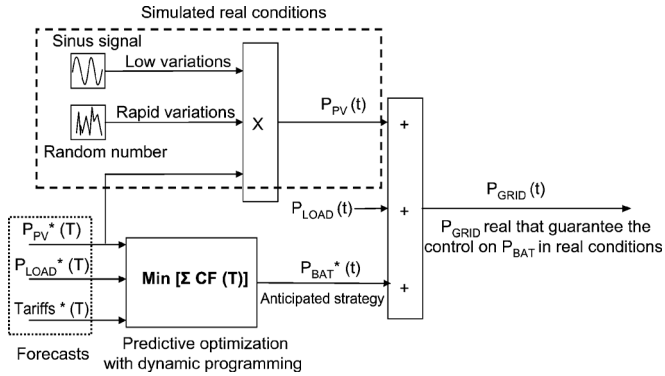

Fig. 13. Scheme of the application of the predictive strategy in real conditions.

B. Application in Real Time and Real Conditions

When the model is executed in the microcontroller, it first computes the predictive optimization stage (the DP algorithm) to obtain the anticipative strategy to apply over the next 24 hours (schedule of the power to exchange with the batteries). Then, the anticipative strategy is applied in the simulated real conditions. The power exchanged with the grid on these new conditions is obtained from the power balance (1). The anticipated scheduling on "P_{BAT}" is applied whatever the real conditions such as physical constraints (3) and (4) are guaranteed even if the peak shaving constraint (5) on "P_{GRID}" is not. A scheme of the application of the predictive strategy in simulated real conditions is presented in Fig. 13. As shown on this figure, the "artificial" perturbations on PV are considered of two natures:

1) Global error on the daily production according to the forecasts. This error is due from the imperfect and approximate forecasts on the meteorological data used to predict the PV production over the day. This is a "low frequency" perturbation. In real cases, this error is generally in the range from 10% to 20%. Generally, the error on the daily PV production is low but the pattern of the production profile is different than expected. This perturbation is created by multiplying the predictive PV production by a factor that varies from 0.6 to 1.4 as a sinus function during the daily PV production period. In this way, the pattern of the PV production profile is modified but the error on the daily production is in the range of the considered perturbation.
2) Local error on the power with rapid variations. This perturbation is due from the clouds or such other inescapable and fast perturbations on the PV power. This is a "high-frequency" perturbation. This error is created by multiplying the predictive PV power by a random factor that varies as a Gaussian distribution around 1 with a variance of 0.01. The sample time for this perturbation is 10 s.

The real-time application has been performed for the 22nd of February as the same day as the simulation results above. For a question of time, as the bench test operates in real time and the perturbations are related only to the PV power, the experiment

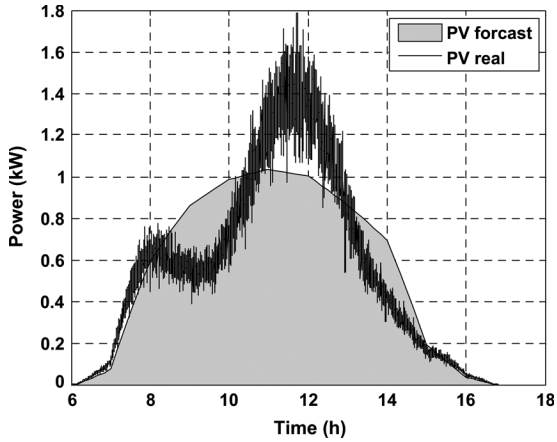

Fig. 14. Comparison between the forecasted and the real PV power for the 22nd of February.

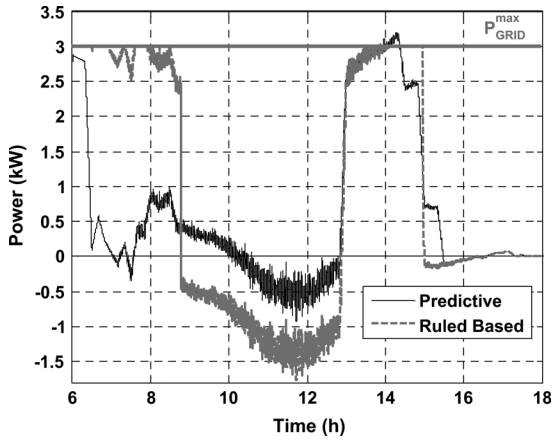

Fig. 15. Profiles of power exchanged with the grid in real conditions for application of the predictive strategy and rule-based strategy for the 22nd of February.

has been performed only for the duration of 12 hours from hours 6 to 18. Fig. 14 compares the forecast of the PV power used to calculate the predictive strategy and the real PV power after applying the artificial perturbations. On this figure, the rapid and local variations as the low variations on the global production from the sinus signal are clearly visible.

C. Experimental Results and Discussions

An important remark is that all the algorithms and strategies presented in this paper, including the optimal predictive algorithm, can be implemented into a microcontroller and executed in real time and in real conditions. The modifications are to translate the algorithms, initially in Matlab format, into a lower level language understandable by the microcontroller. This is a significant result as an issue to a rapid industrial development.

The power exchanges with the grid from application of the predictive strategy and ruled-based strategy in real conditions and real time are presented on Fig. 15. The SOC of batteries are compared in Fig. 16. According to the method of application, the SOC profile for the predictive strategy in real condition is the same as the one anticipated and presented in Fig. 10. The load profile is not presented as the same as the one in Fig. 9.

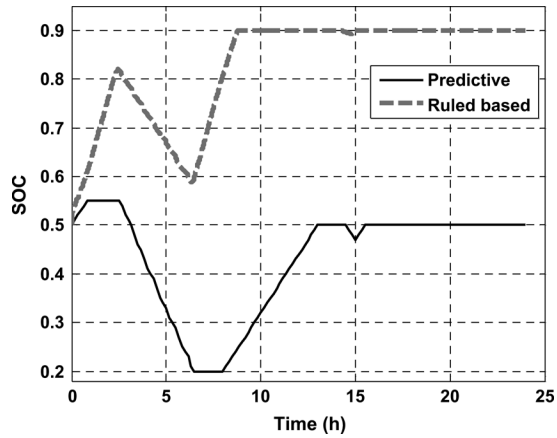

Fig. 16. Profiles of SOC of batteries in real conditions for application of the predictive strategy and rule-based strategy for the 22nd of February.

As expected when the predictive strategy is applied in real conditions, the anticipated schedule is followed since there is no perturbation (Fig. 15). As the predictive power of batteries is imposed, in real conditions the perturbations are balanced on the power exchanged with the grid. As observed in Fig. 15, all the rapid variations appear on the power exchanged with the grid and when the PV power is higher than predicted, more power is injected into the grid. In the same way, when the PV power is lower than anticipated, the grid supplies more power. In real conditions, this mode of operation does not guaranty the peak shaving constraint (5) on "P_{GRID}", as observed on Fig. 15 around 14:30.

For the ruled-based strategy, the constraint on the power exchanged with the grid in real conditions is always guaranteed. However and as expected, the equality constraint on the initial and final SOC of batteries is not respected. As shown on Fig. 16, batteries are fully charged at the end of the day which restricts the flexibility of the management of the next day. Also and as remarked before, use of the PV power is not optimized as it is mainly used to feed the grid instead of charging the batteries. In this way, the objective function is also not optimized. The ruled-based algorithm is the easiest one to implement and to develop at an industrial scale but it does not reach the objective and it limits the flexibility of a day-to-day management. In this consideration, the ruled-based algorithm does not present interests for our study and has been used only as a reference for comparison with the strategy proposed.

Theses results and comparisons lead to the reflection about the type of control to apply in real conditions to guaranty all the constraints and in the ideal case why not also to guaranty optimality according to the real conditions and the objective function. The question of performing a new predictive optimization from updates forecast can also be asked.

Finally, it is carried out that the management in real conditions is strongly dependent on the accuracy of the forecasts and on the reactive mode of operation that is applied. However, predictive optimization is a necessary stage to reach the final objective of optimal management in real conditions. In this consideration, a significant step has been achieved implementing the predictive algorithm into a microcontroller to real-time execution.

VII. Conclusion and Future Work

In this paper, a predictive control system based on a DP approach, that optimizes the power flow management into a grid connected PV system with storage, has been presented. According to the power supervisor proposed in Section II-C, the study focuses on predictive optimization from "*a priori*" known forecasts. The objective was to perform peak shaving with the lower cost for the owner of the system. The particularity of the approach lies in the consideration of the batteries' ageing into the day-ahead power management.

Simulations and real-time operation in simulated real conditions have been performed and results compared with a ruled-based management. In simulation over 24 hours, predictive optimization provides around 13% of gain on the electricity bill for the economical context of the study. Implementation of the predictive optimization algorithm into a microcontroller to perform real-time management figured out the industrial potentiality of the method proposed. Operation of the management in real conditions has validated the results and assumptions from simulations. Performances of the management in real conditions strongly depend of the accuracy of the forecasts and of the mode of operation. This important conclusion leads to many questions about reactive power management without denying the importance and the necessity of the predictive optimization stage.

The management developed helps integration of PV power into the grid as peak loads are shaved. Depending of the reactive management in real conditions, the power fluctuation of the PV production is balanced to the power exchanged with the grid or with the batteries. In this context, next and future works will deal with reactive management for real condition operations. From the conclusion of this study, a different reactive management will be developed and compared in real condition operations. Specifically, an optimal reactive management, developed from the DP algorithm of the predictive optimization stage, will be proposed. In this way, the sum of the works will achieved to a complete power management system that is reactive such as optimal management is guaranteed according to the real conditions.

References

[1] Trends in Photovoltaic Applications. Survey Report of Selected IEA Countries Between 1992 and 2007 IEA Photovoltaic Power Systems Program, IEA PVPS T1-17, 2008.

[2] A. Woyte, V. Van Thong, R. Belmans, and J. Nijs, "Voltage fluctuations on distribution level introduced by photovoltaic systems," *IEEE Trans. Energy Convers.*, vol. 21, no. 1, pp. 202–209, Mar. 2006.

[3] P. Denholma and R. M. Margolis, "Evaluating the limits of solar photovoltaics next term (PV) in traditional electric power systems," *Energy Policy*, vol. 35, pp. 2852–2861, 2007.

[4] P. Denholma and R. M. Margolis, "Evaluating the limits of solar photovoltaics (PV) in electric power systems utilizing energy storage and other enabling technologies," *Energy Policy*, vol. 35, pp. 4424–4433, 2007.

[5] M. Perrin, Y. M. Saint-Drenan, F. Mattera, and P. Malbranche, "Lead-acid batteries in stationary applications: Competitors and new markets for large penetration of renewable energies," *J. Power Sources*, vol. 144, pp. 402–410, 2005.

[6] J. M. Eeyer, J. J. Jannucci, and G. P. Corey, Energy Storage Benefits and Market Analysis Handbook, A Study for the DOE Energy Storage Systems Program, Sandia Report Sandia National Laboratories, 2004.

[7] G. Bundestag, Update of Feed in Tariff for Renewable Energies in Germany Feed in International Corporation, 2008.

[8] A. M. Kalogirou, "Artificial intelligence techniques for photovoltaic applications: A review," *Prog. Energy Combustion Sci.*, vol. 38, pp. 574–632, 2008.

[9] F. Fusco and J. V. Ringwood, "Short-term wave forecasting for real-time control of wave energy converters," *IEEE Trans. Sustainable Energy*, vol. 1, no. 2, pp. 66–106, Jul. 2010.

[10] M. Ceraolo, A. Di Donato, and G. Franceschi, "A general approach to energy optimization of hybrid electric vehicles," *IEEE Trans. Veh. Technol.*, vol. 57, no. 3, pp. 1433–1441, May 2008.

[11] C. Wang and M. H. Nehrir, "Power management of a stand-alone wind/photovoltaic/fuel cell energy system," *IEEE Trans. Energy Convers.*, vol. 23, no. 3, pp. 957–967, Sep. 2008.

[12] K. Agbossou, M. Kolhe, J. Hamelin, and T. K. Bose, "Performance of a stand-alone renewable energy system based on energy storage as hydrogen," *IEEE Trans. Energy Convers.*, vol. 19, no. 3, pp. 633–640, Sep. 2004.

[13] S. Jain and V. Agarwal, "An integrated hybrid power supply for distributed generation application fed by nonconventional energy sources," *IEEE Trans. Energy Convers.*, vol. 23, no. 2, pp. 622–634, Jun. 2008.

[14] M. Urbina and Z. Li, "A fuzzy optimization approach to PV/battery scheduling with uncertainty in PV generation," in *Proc. 38th North American IEEE Power Symp. (NAPS 2006)*, Carbondale, IL, 2006, pp. 561–566.

[15] A. W. Yang, "Design of energy management strategy in hybrid vehicles by evolutionary fuzzy system part I: Fuzzy logic controller development," in *Proc. 6th World Congress on Intelligent Control and Automation*, Dalian, China, Jun. 21–23, 2006.

[16] A. Borghetti, C. D'Ambrosio, A. Lodi, and S. Martello, "An MILP approach for short-term hydro scheduling and unit commitment with head-dependent reservoir," *IEEE Trans. Power Syst.*, vol. 23, no. 3, pp. 1115–1124, Aug. 2008.

[17] T. T. Ha Pham, F. Wurtz, and S. Bacha, "Optimal operation of a PV based multi-source system and energy management for household application," in *Proc. IEEE Int. Conf. Industrial Technology (ICIT)*, Gippsland, Victoria, Australia, 2009, pp. 1–5.

[18] B. Lu and M. Shahidehpour, "Short term scheduling of battery in a grid connected PV/battery system," *IEEE Trans. Power Syst.*, vol. 20, no. 2, pp. 1053–1061, May 2005.

[19] A. G. Bakirtzis and P. S. Dokopoulos, "Short term generation scheduling in a small autonomous system with unconventional energy sources," *IEEE Trans. Power Syst.*, vol. 3, no. 3, pp. 1230–1236, Aug. 1988.

[20] Q. Gong, Y. Li, and Z.-R. Peng, "Trip-based optimal power management of plug-in hybrid electric vehicles," *IEEE Trans. Veh. Technol.*, vol. 57, no. 6, pp. 3393–3401, Nov. 2008.

[21] M. Koot, J. T. B. A. Kessels, B. de Jager, W. P. M. H. Heemels, P. P. J. Van Den Bosch, and M. Steinbuch, "Energy management strategies for vehicular electric power systems," *IEEE Trans. Veh. Technol.*, vol. 54, no. 3, pp. 771–782, May 2005.

[22] F. Besnard and L. Bertling, "An approach for condition-based maintenance optimization applied to wind turbine blades," *IEEE Trans. Sustainable Energy*, vol. 1, no. 2, pp. 77–83, Jul. 2010.

[23] J. T. B. A. Kessels, M. Koot, B. de Jager, P. P. J. Van Den Bosch, N. P. I. Aneke, and D. B. Kok, "Energy management for the electric powernet in vehicles with a conventional drivetrain," *IEEE Trans. Control Syst. Technol.*, vol. 15, no. 3, pp. 494–505, May 2007.

[24] J. T. B. A. Kessels, M. W. T. Koot, P. P. J. Van Den Bosch, and D. B. Kok, "Online energy management for hybrid electric vehicles," *IEEE Trans. Veh. Technol.*, vol. 57, no. 6, pp. 3428–3440, Nov. 2008.

[25] E. Skoplaki and J. A. Palyvos, "On the temperature dependence of photovoltaic module electrical performance: A review of efficiency/power correlations," *Solar Energy*, to be published.

[26] A. Luque and S. Hegedus, *Handbook of Photovoltaic Science and Engineering*. Hoboken, NJ: Wiley, 2003, pp. 943–951.

[27] M. Ceraolo, "New dynamical models of lead-acid batteries," *IEEE Trans. Power Syst.*, vol. 15, no. 4, pp. 1184–1190, Nov. 2000.

[28] C. A. Shepherd, "Design of primary and secondary ceils—II. An equation describing battery discharge," *J. Electrochem. Soc.*, vol. 112, no. 7, pp. 657–664, 1965.

[29] J. B. Copetti, E. Lorenzo, and F. Chenlo, "A general battery model for PV systm simulation," *Prog. Photovoltaics, Res. Applicat.*, vol. 1, pp. 283–292, 1993.

[30] A. Delaille, F. Huet, E. Lemaire, F. Mattera, M. Perrin, and M. Vervaart, "Development of a battery fuel gauge based on ampere-hour counting," in *Proc. 21st Eur. Photovoltaic Solar Energy Conf.*, Dresden, Germany, Sep. 4–8, 2006.

[31] A. Delaille, Development of New State-of-Charge and State-of-Health Criteria for Batteries Used in Photovoltaic Systems University Pierre et Marie Curie, Ph.D Report (French), 2006.
[32] Y. Riffonneau, A. Delaille, F. Barruel, and S. Bacha, "System modeling and energy management for grid connected PV systems with storage," in *Proc. 24th EU Photovoltaic Solar Energy Conf.*, Valencia, Spain, 2008.
[33] E. Lemaire-Potteau, F. Mattera, A. Delaille, and P. Malbranche, "Assessment of storage ageing in different types of PV systems technical and economical aspects," in *Proc. 24th EU Photovoltaic Solar Energy Conf.*, Valencia, Spain, 2008.
[34] Y. Guoa, S. Tang, G. Meng, and S. Yang, "Failure modes of valve regulated lead acid batteires for electric bicle application in deep disscharge," *J. Power Sources*, vol. 191, pp. 127–133, 2009.
[35] S. Hua, Q. Zhou, D. Kong, and J. Ma, "Application of valve-regulated lead-acid batteries for storage of solar electricity in stand-alone photovoltaic systems in the northwest areas of china," *J. Power Sources*, vol. 158, pp. 1178–1185, 2006.
[36] M. Vervaart, Test of a Photovoltaic Inverter of a Rated Power of 1100 W INES institute, 2007.
[37] R. Bellman, "The theory of dynamic programming," *RAND Corporation, Proc. National Academy of Sciences*, pp. 503–715, 1952.
[38] A. Kauffman, "Méthodes et modèle de la recherche opérationnelle," *L'économie d'entreprise, tom 1 & 2,* , vol. 10, Dunod, 1968.
[39] C. Venu, Y. Riffonneau, S. Bacha, and Y. Baghzouz, "Battery storage system sizing in distribution feeders with distributed photovoltaic systems," in *Proc. IEEE Powertech Conf.*, Roumania, Bucarest, 2009.
[40] RT-Lab Sep. 2010 [Online]. Available: http://www.opal-rt.com/product/rt-lab-professional
[41] O. Craciun, A. Florescu, S. Bacha, I. Munteanu, and A. Iuliana Bratcu, "Hardware-in-the-loop testing of PV control systems using RT-Lab simulator," in *Proc. 14th Int. EPE Power Electronics and Motion Control Conf. (EPE-PEMC)*, Ohrid, Republic of Macedonia, 2009.

Yann Riffonneau was born in Tours, France, in 1983. He received the Master's degree in renewable energy in 2006 from Savoir University and the Ph.D. degree in electrical engineering from Joseph Fourirer University of Grenoble in 2009.

He is currently doing postdoctoral work at G2Elab, St. Martin d'Hères, France, on energy management in multipower sources building at G2Elab. His fields of interest include energy management, optimization, quality of power, and renewable energy.

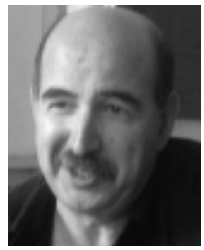

Seddik Bacha (M'08) received the Engineer and Magister degrees from École Nationale Polytechnique de Algiers, Algeria, in 1982 and 1990, respectively, and the Ph.D. degree from Institut National Polytechnique de Grenoble, France, in 1993.

He joined the Laboratoire d'Electrotechnique de Grenoble (LEG) in 1990 and in 1998 he was habilitated to conduct research. He is currently Manager of the Power Systems Group with Grenoble Electrical Engineering Laboratory (G2ELab) and a Professor with the Joseph Fourier University of Grenoble. His research interests include power electronics system modeling and control, power quality, and renewable energy integration.

Franck Barruel received the Engineer and Magister degrees from Ecole Nationale Supérieure d'Ingéieurs Ilectriciens de Grenoble-France, in 2002, and the Ph.D. degree from Joseph Fourier University, in the Laboratoire d'Electrotechnique de Grenoble (LEG), in 2005.

He joined the Commissariat à l'Energie Atomique et aux Energies Alternatives (CEA) in the French National Solar Institut (INES) in 2006. He is a specialist in solar system modeling, energy flow management, and is involved in the solar mobility concept.

Stephane Ploix received an Engineer degree in mechanics and electricity, and the Ph.D. degree in control engineering and signal processing from the Institut National Polytechnique de Lorraine, in 1998.

He is Maître de Conférences at the Grenoble Institute of Technology, Grenoble, France, in the G-SCOP Laboratory. He is a specialist in supervision, monitoring and diagnosis and his studies focus on human-machine cooperative mechanisms. He is involved in different industrial projects dealing with supervision of distributed plants, diagnosis of human skills, iterative diagnosis tool for companies, and power management in buildings.